Journal of Nanoscience and Nanoengineering
Vol. 5, No. 3, 2019, pp. 16-24
http://www.aiscience.org/journal/jnn
ISSN: 2471-8378 (Print); ISSN: 2471-8394 (Online)

Preparation and Characterization of ZnO/TiO_2 Composite Nanomaterial Using Low Temperature Synthesis Method

Rasha Adam Shommein[1, *], Suhair Kamaleldin Shomeina[2], Omer Nur[3], Mustafa Abbas Mustafa[4]

[1]Department of Appropriate Technology and Urban Development, Institute of Engineering Research & Materials Technology, National Centre for Research, Khartoum, Sudan
[2]Department of Chemicals and Cellulose, Institute of Engineering Research & Materials Technology, National Centre for Research, Khartoum, Sudan
[3]Department of Physics and Technology, Linköping University, Linköping, Sweden
[4]Materials and Nanotechnology Research Centre, University of Khartoum, Khartoum, Sudan

Abstract

Nanotechnology is one of the new methods technologies, which can use bottom- up approach with low temperature chemical growth to synthesize nanomaterial particle. There are diverse aspects of the preparation and characterization of nanoscopic ZnO, and composite ZnO/TiO_2 materials. In this study, ZnO NPs were prepared by hydrothermal method, using 1: 1.5 ratio of Zinc acetate diyhdrate to Sodium hydroxide. Then prepared ZnO NPs were used with commercial rutile TiO_2 NPs a mean diameter about 40 nm, to prepare composite ZnO/TiO_2 NPs with ratio 1: 3, which were successfully synthesized by modified hydrothermal method. Different techniques used to investigate the crystal structure, morphology, the chemical composition, UV-visible, and energy band gap of NPs. The XRD confirms that the formation of rutile TiO_2 and zincite ZnO NPs phases in the composite structure; the observation shows according to SEM images, ZnO NPs have hexagonal shapes; TiO_2 NPs have a tetragonal shape, and ZnO/TiO_2 composite present as cubic NPs shape. Also the (EDS) observation shows availability of ZnO, TiO_2 and composite ZnO/TiO_2 NPs in the sample; and UV-visible light confirms the wavelength range and band gap energy of ZnO, TiO_2 and composite ZnO/TiO_2 NPs.

Keywords

Nanoparticles (NPs), Titanium Oxide (TiO_2), Zinc Oxide (ZnO), Composite (ZnO/TiO_2), X-Rays Diffraction (XRD), Characterization

Received: September 11, 2019 / Accepted: October 31, 2019 / Published online: December 5, 2019

1. Introduction

Nanotechnology deals with structures with a size range of 1 to 100 nm at least in one dimension, the positive impact of nanotechnology is increasing in all areas of science and technology [1]. Nanotechnology is associated with material, devices, machines with small size [2], and it can use bottom-up approach or top down approach to synthesize particle. Developing countries can use bottom up approach technique, because it need low temperature to make chemical growth.

TiO_2, ZnO are nanomaterials at a nanoscale level, which are produced by low cost, good chemical stability, and can be acquired using low temperature synthesis [3]. Also they have similar physical properties and almost the same large band gap energies (~3.2 eV) [4], ZnO has higher absorption efficiency across a larger fraction of solar spectrum

* Corresponding author
E-mail address: rasha-80@hotmail.com (R. A. Shommein), rshummein@gmail.com (R. A. Shommein)

compared to TiO_2 [5].

Recent years have an exponential growth and wide attention of publications on the preparation and characterization of nanomaterials [3]. TiO_2 have various chemical forms that can be classified into the typical TiO_2 and Ti_nO_{2n-1} form, and possess varying crystalline phases, including tetragonal, orthorhombic, monoclinic, hexagonal, triclinic, and rhombohedra crystals, but it can mainly be sorted into four crystalline structures of rutile (tetragonal structure), anatase (tetragonal structure), brookite (orthorhombic structure), and TiO_2 (B) (monoclinic) [6, 7]. TiO_2 is thermally stable, non-toxic, inert versus acids, safe pigment, alkalis and solvents, and insoluble in water [2].

It can be prepared in various syntheses as hydrothermal method, sol-gel method, solvothermal method, and hydrolysis and condensation method. TiO_2 NPs are also used for a large variety of applications such as self-cleaning, self-sterilizing solid surfaces, water purification [2], wastewater dyes degradation [8], air purification, antifogging effect, cosmetics, pharmaceutical, paper industry [2], photo-degradation of organic compounds [5], toothpaste, paints, coatings [9], photovoltaics, gas sensors, and dye sensitized solar cell [10].

ZnO NPs have been employed in a number of arising applications, such as sunscreens, coatings, paint, antibacterial creams, cosmetics, deodorant, self-cleaning [9], air purification [6], mouthwash, solar and UV disinfection of water and wastewater, reactive membranes, biofouling-resistant surfaces, biofouling-resistant membranes, carbon hollow fibers, packed bed filters hollow fibers [9], gas and humidity sensors, UV detectors, and optoelectronic devices [10].

ZnO nanostructures can be syntheses by sundry methods hydrothermal (chosen method for this study), electrochemical deposition, sol-gel, precipitation, microemulsion, solvothermal, microwave, wet chemical method, chemical path deposition, flux methods and electrospinning. The growth of ZnO nanostructures can be nanoparticles, nanowires, nanotube, nanosheets, nanorods [4], nanoneedles, nanoflowers, nanofibres, and nano-thin film. ZnO can form a crystal in three different forms: hexagonal wurtzite, cubic zincblende and rocksalt. ZnO hexagonal wurtzite is thermodynamically but it can bestable at ambient conditions, cubic zincblende can be stabilized by growing ZnO on cubic substrates, ZnO can exist in the rocksalt structure only at relatively high pressures [5].

Composite and doping material has been adopted to modify the physical and chemical properties of ZnO or TiO_2, by incorporating impurities such as metals or non-metals. The doping formation of nano-composites, noble metal and non-noble metal deposition have been made toward extending photoactivity of TiO_2 in visible light region [7]. There are various ways used to reduce the band gap, and increase the photoactivity of TiO_2, one of them it's doping with different metal ions and oxides, such as composite or doping TiO_2 with ZnO. On the other hand, particle morphology of the TiO_2 was affected by the addition of ZnO, and the size distribution of ZnO/TiO_2 nano-composite was improved with increasing ZnO molar ratio [8].

In the last years, composite ZnO/TiO_2 NPs present high interest due to it's a large range of applications, such as semiconductor film for photo anode of dye sensitized solar cell [4], optoelectronic device, and photocatalytic [10]. Composite ZnO/TiO_2 NPs have different methods to synthesis, such aswet chemical method, sol–gel method, fast–dip–coating method, atomic layer deposition technique, dipping-rinse-hydrolyzation process [4], including thermal chemical vapor deposition, radio frequency magnetron sputtering, spray pyrolysis [8], and hydrothermal method which chosen to be used in this study, according to its low temperature used to synthesis particles and easily controlled reaction conditions. [7]

2. Materials and Methods

2.1. Materials

Zinc Acetate dehydrate ($Zn(CH_3COO)_2.2H_2O$) 98% extra pure (LOBA Chemie PVT. LTD.), Sodium Hydroxide (NaOH) pellets purified (CDH), TiO_2 Nanomaterial (T104938-100 g, rutile, 99.8% metals basis, 40 nm) was purchased from Aladdin industrial corporation (China); and nitric acid (HNO_3 69%) extra pure (LOBA Chemie PVT. LTD.) was used to control the pH, absolute ethanol 96% and deionized water were used to synthesis processes.

2.2. Methodology

2.2.1. Synthesis of ZnO NPs by Hydrothermal Method

ZnO NPs was prepared by hydrothermal method; with ratio 1.5:1 of Zinc Acetate dehydrate to Sodium Hydroxide. 0.05 M Zinc acetate was prepared in deionized water, and stirred for a few minutes to produce solution (A), 0.05 M NaOH was prepared in deionized water to produce solution (B), adding solution (B) to solution (A) drop wise under continuous stirring 350 rpm with magnetic rod until clear solution was obtained, then the resulted solution was heated at 60 °C with continuous stirring for 2 hours.

2.2.2. Synthesis of ZnO/TiO_2 Composite NPs by Modified Hydrothermal Method

To prepare ZnO/TiO_2 composite NPs with ratio 1:3 of ZnO

NPs to TiO_2 NPs, there was modified method used to prepare TiO_2 solution [10]; by stoichiometric calculation to find the exact amount of TiO_2 that can be used. 1.5 gm of TiO_2 was dissolved in 50 ml ethanol with stirring for a few minutes at room temperature, and then 0.5 gm of prepared ZnO NPs was added to the solution. The mixture was stirred vigorously with magnetic stirrer for 30 minutes, followed by addition of 1 ml H_2O for hydrolysis, then drops wisely 0.8 ml of HNO_3 was added to control the pH (pH at start 7.19- pH in the end 4.5). The solution was heated at 220°C under continuous stirring for 20 minutes; the final product was filtrated, washed with ethanol and dried in an oven at 80°C for 15 minutes.

3. Results and Discussion

The morphology, crystal structure, elemental chemistry composition, and size of ZnO, TiO_2, and composite ZnO/TiO_2 NPs, were investigated by a scanning electron microscope (SEM) (MIRA3 TESCAN performance in nanospace, Oxford, Germany), X-ray diffraction (XRD) (Shimadzu XRD-7000 X-ray diffractometer instrument, Hitachi corporation, Japan) using zirconium (Zr) tube, energy dispersive X-ray spectrometer (EDS), and UV-visible spectrophotometer (Shimadzu UV-vis- 1800, Hitachi corporation, Japan).

3.1. XRD Analysis of ZnO, TiO_2, and Composite ZnO/TiO_2 NPs

ZnO NPs phase compositions were determined by XRD, using Cu-Ka1 radiation (λ=1.540600 Å) with space group of P 63 m c, and unit cell (a=3.2490 Å c=5.2070 Å). The peaks are consistent of hexagonal wurtzite structure, and the chemical composition shows the characteristic X-ray energy level sequence Zincite, the particle distance (D) was ranged between (1.2380- 2.8061) Å, 2-Theta (2θ) angle was ranged between (31.88- 76.95)°, the average crystallite size calculated from selected peaks/lines was 1110.0 Å or 111 nm, and crystallite size estimated by using Scherrer's formula:

$$B(2\theta) = \frac{K\lambda}{L\cos\theta} \quad (1)$$

B: is Peak width inversely proportional to crystallite size (L).

K: the Scherrer constant.

θ: is Bragg diffraction angle.

λ: is wavelength.

When Scherrer's constant used in calculation is 0.94.

$$B(2\theta) = \frac{0.94\,\lambda}{L\cos\theta} \quad (2)$$

the crystalline sizes of ZnO NPs was range between (109–134) nm, Figure 1 showing ZnO NPs main peaks were at 2θ=31.88°, 34.52°, 36.36°, 47.62°, 56.68°, and 62.95°, which corresponding to (100), (002), (101), (110), (103), and (112) crystal lattice planes of ZnO respectively, that according to Joint Committee on Powder Diffraction Standards (JCPDS) database card JCPDS PDF no. 36-1451 [11, 12], the strong characteristic diffraction peaks (100), (002), and (101) showing in Figure 2.

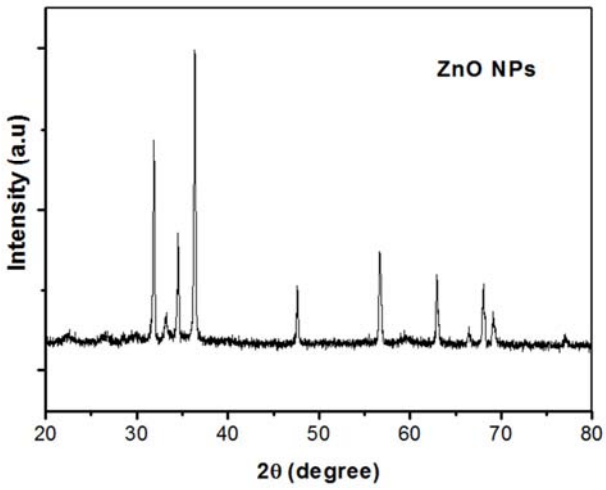

Figure 1. XRD pattern of ZnO NPs.

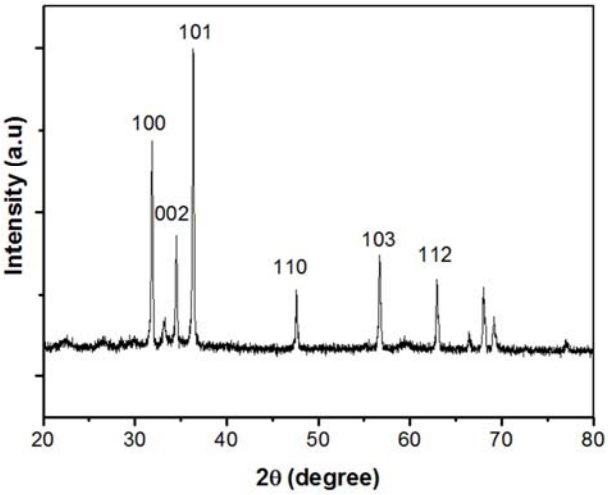

Figure 2. XRD pattern of ZnO NPs crystal lattice planes.

For TiO_2 NPs type rutile the crystal system is tetragonal, using Cu-Ka1 radiation (λ=1.540600 Å) with space group of P 42/m n m, and unit cell (a=4.5930 Å, c=2.9590 Å), The chemical composition shows the characteristic X-ray energy level sequence titanium, D was ranged between (1.2414-3.2358) Å, 2θ was ranged (27.54- 76.70)°, the crystallite size estimation using Scherrer's formula, when Scherrer's constant used in calculation is 0.94 (formula 2), showing that TiO_2 NPs crystalline sizes was range between (51.94- 64.33) nm, and average crystallite size calculated from selected peaks/lines was 535.6 Å or 53.56 nm, Figure 3 showing the

main peaks of TiO_2 NP were at 2θ=27.54°, 36.20°, 41.36°, 54.43°, 56.77°and 69.08°, which corresponding to (110), (101), (111), (211), (310) and (301) crystal lattice planes of ZnO, respectively, the strong characteristic diffraction peaks (110), (101), and (211) showing in Figure 4, these peaks are consistent with the TiO_2 rutile database [13].

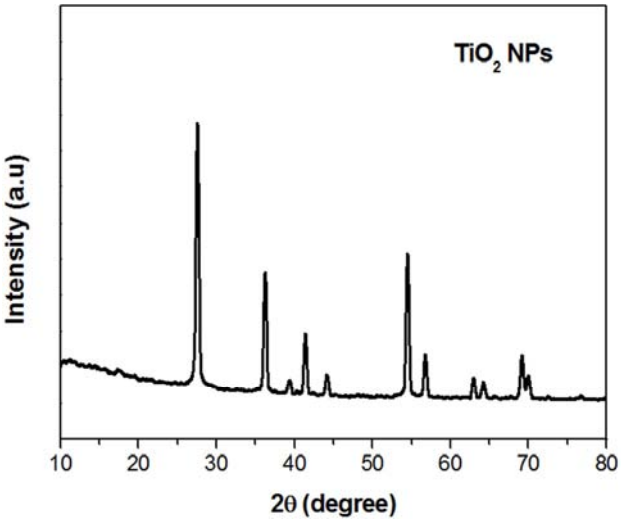

Figure 3. XRD pattern of TiO_2 NPs.

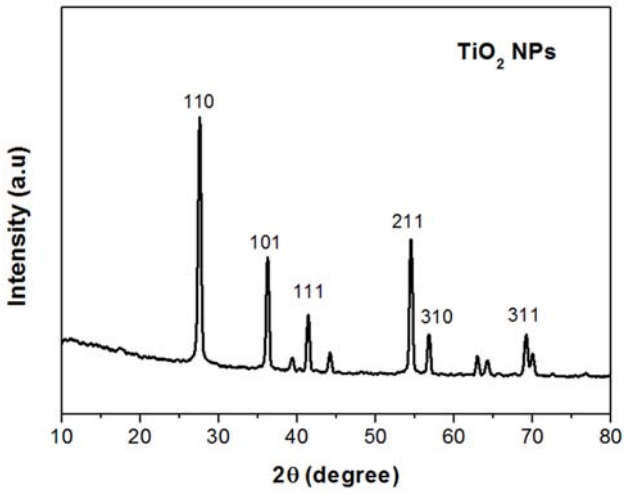

Figure 4. XRD pattern of TiO_2 NPs crystal lattice planes.

The crystal system of composite ZnO/TiO_2 NPs was cubic using Cu-Ka1 radiation (λ=1.540600 Å) with space group of F d -3 m, and unit cell a=8.4450 Å. D was ranged between (1.2872- 4.8808) Å, 2θ was ranged (18.16- 73.51)°, Figure 5 presents the main peaks of composite ZnO/TiO_2 NPs were at 2θ=18.16°, 27.72°, 36.88°, 41.57°, 54.60°, and 57.56°, which corresponding to (100), (110), (101), (111), (211), and (301) crystal lattice planes of ZnO/TiO_2 NPs [14], the strong characteristic diffraction peaks (110), (101), and (211) showing in Figure 6.

Procedure of TiO_2 NPs mixed with the ZnO NPs was performed by XRD analyses of the composite NPs. The corresponding XRD patterns showed both TiO_2 peaks and ZnO wurtzite structure, TiO_2 atoms can be incorporated into the ZnO lattice by substitution process, showing in Figure 7.

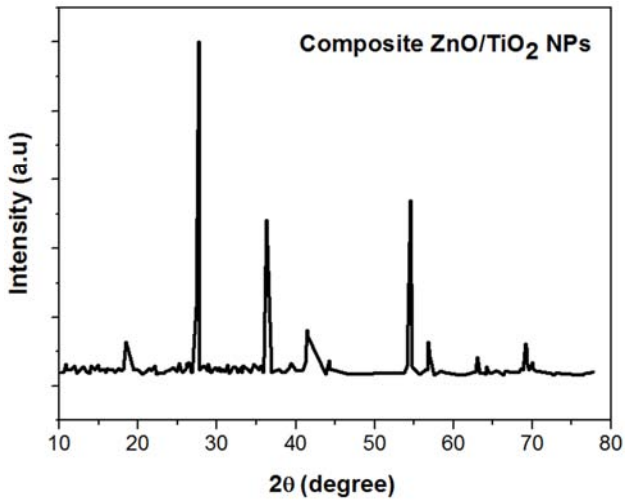

Figure 5. XRD pattern of composite ZnO/TiO_2 NPs peaks.

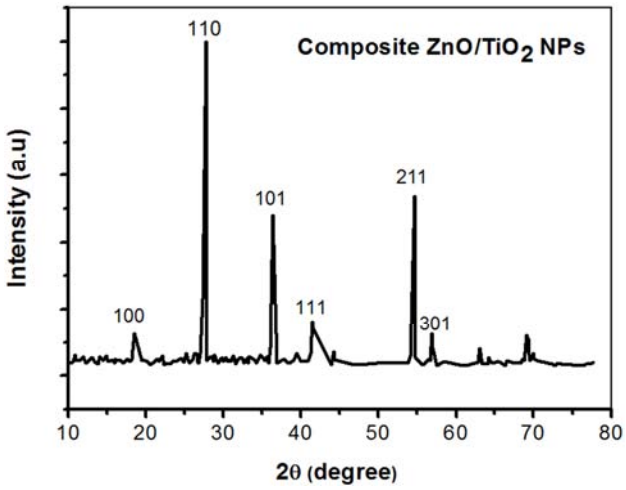

Figure 6. XRD pattern of composite ZnO/TiO_2 NPs crystal lattice planes.

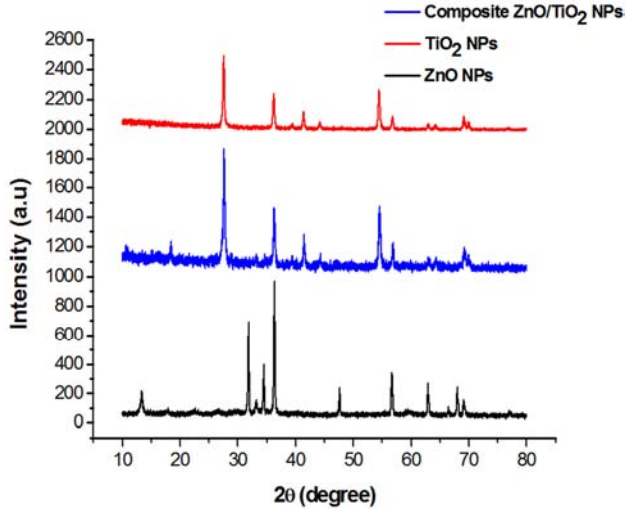

Figure 7. XRD pattern of comparing NPs peaks.

3.2. SEM Analysis of ZnO, TiO_2, and Composite ZnO/TiO_2 NPs

The morphological observation shows according to SEM images, that ZnO NPs have hexagonal shapes, and the particle radius (r) or distance (D) ranged between (179-500) nm, showing in Figure 8.

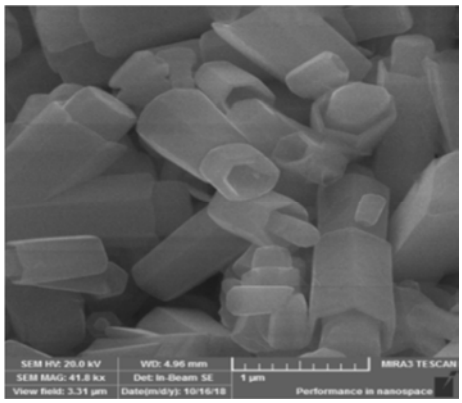

(a)

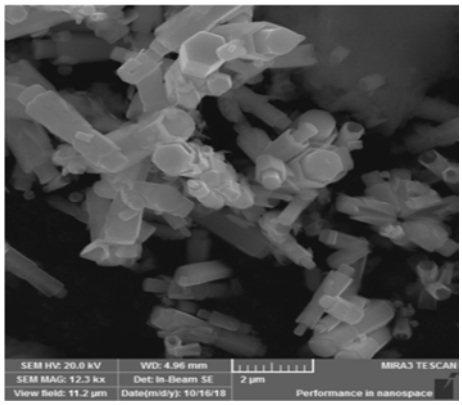

(b)

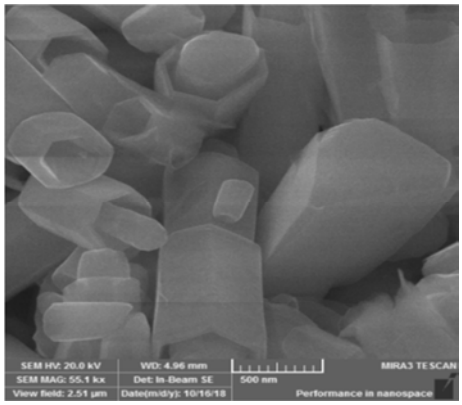

(c) 500 nm.

Figure 8. SEM image of ZnO NPs prepared by the low temperature hydrothermal method, (a) 1µm, (b) 2µm, and (c) 500 nm.

TiO_2 NPs have a tetragonal shape, and the particle (r) and (D) are range between (27- 50) nm, as shown in Figure 9.

Figure 10 presents the shape of composite ZnO/TiO_2 was NPs, while the particle radius (r) and distance (D) range between (36.48- 53) nm.

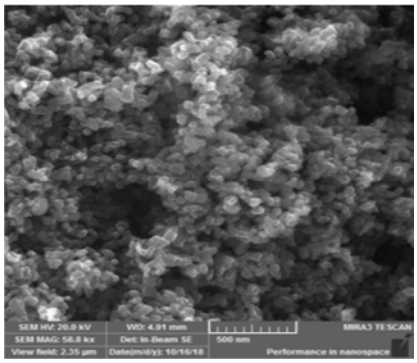

(a)

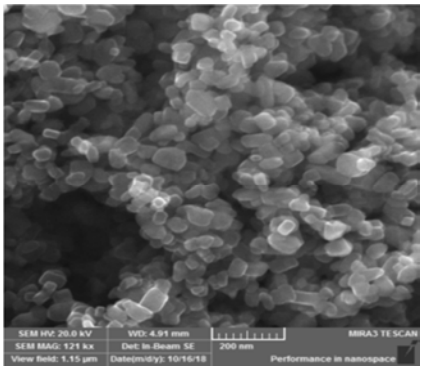

(b)

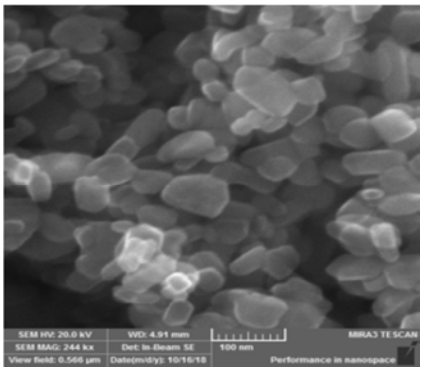

(c)

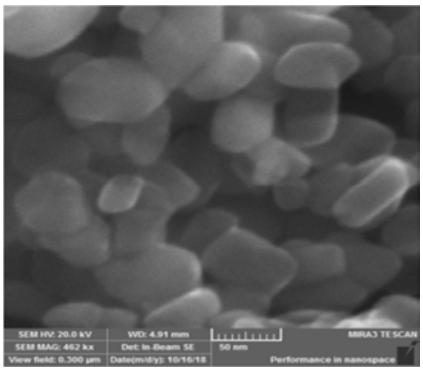

(d)

Figure 9. SEM image of TiO_2 NPs rutile, (a) 500 nm, (b) 200 nm, (c) 100 nm, and (d) 50 nm.

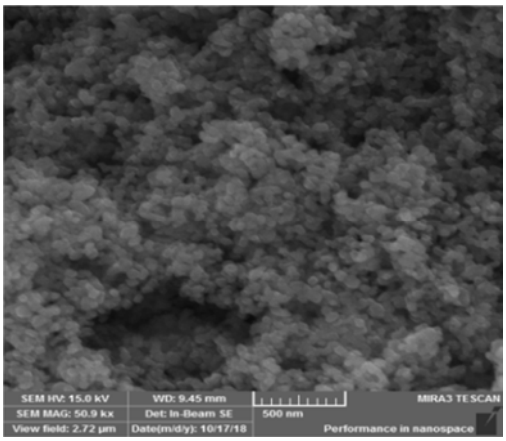

(a)

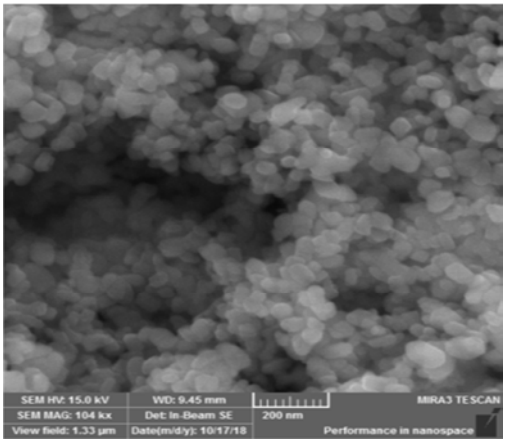

(b)

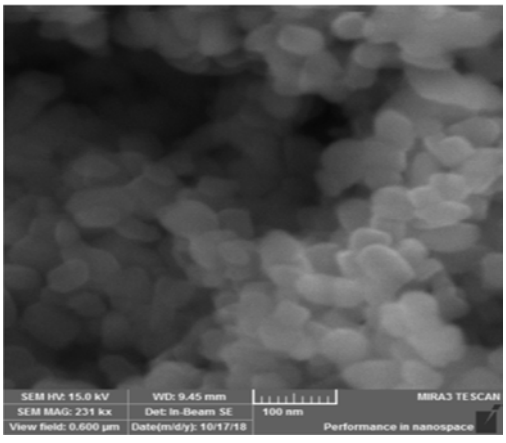

(c)

Figure 10. SEM image of ZnO/TiO_2 composite NPs prepared by the low temperature hydrothermal method, (a) 500 nm, (b) 200 nm, and (c) 100 nm.

3.3. EDX Analysis of ZnO, TiO_2, and Composite ZnO/TiO_2 NPs

The chemical composition was determined by Energy Dispersive X-ray spectroscopy (EDS), using OXFORD instrument, showing ZnO NPs in Figure 11. The presence of Zn, and O was detected and impurities of Na derived from experiment residue.

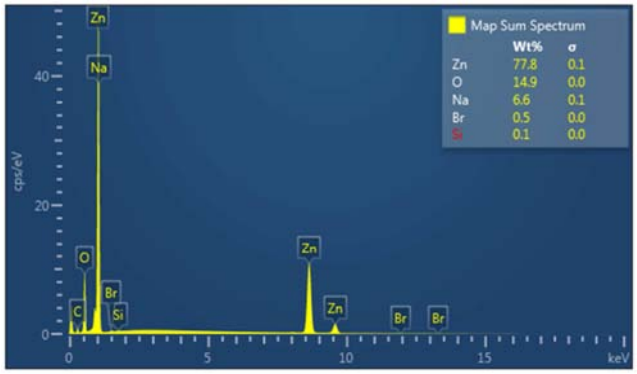

Figure 11. EDS spectra analysis of ZnO NPs.

Figure12 shows EDS spectra analysis of TiO_2 NPs rutile, the presence of Ti, O was detected and impurities are present (Cu derived from EDS, Al derived from experiment covered foil).

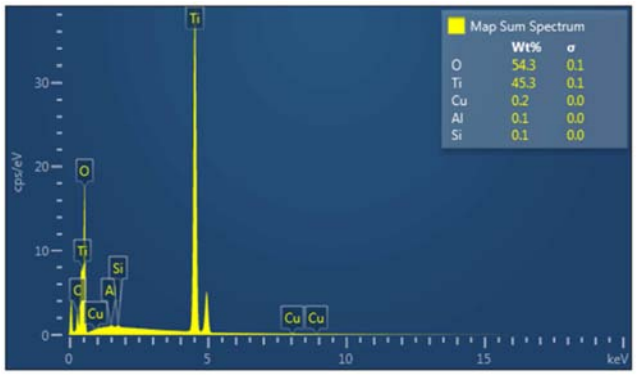

Figure 12. EDS spectra analysis of TiO_2 NPs..

EDS analysis of ZnO/TiO_2 composite NPs presented in Figure 13 the presence of Ti, Zn, O was detected and impurities of (Al derived from experiment covered foil, C derived from EDS tape).

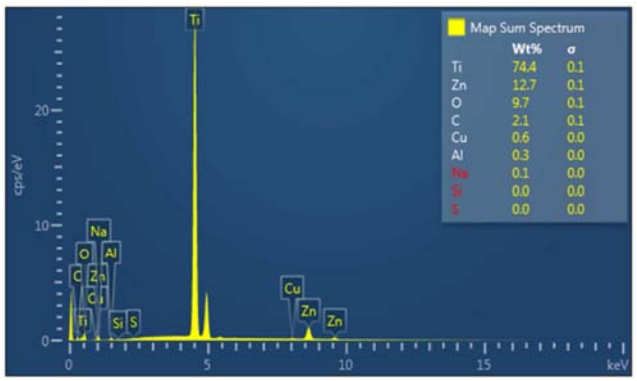

Figure 13. EDS spectra analysis of ZnO/TiO_2 composite NPs.

3.4. UV-visible Spectrophotometer Analysis and Band-gap Energy of ZnO, TiO_2, and Composite ZnO/TiO_2 NPs

UV-visible confirms the wavelength of ZnO, TiO_2 and

composite ZnO/TiO_2 NPs respectively in the samples, by measuring starting absorbance point, maximum peak point (λ_{max}), and last point.

The absorption of ZnO NPs starting in the wavelength 250 nm, calculation show the λ_{max} of ZnO NPs absorbance peak at 550 nm, the last point of absorption at 800 nm.

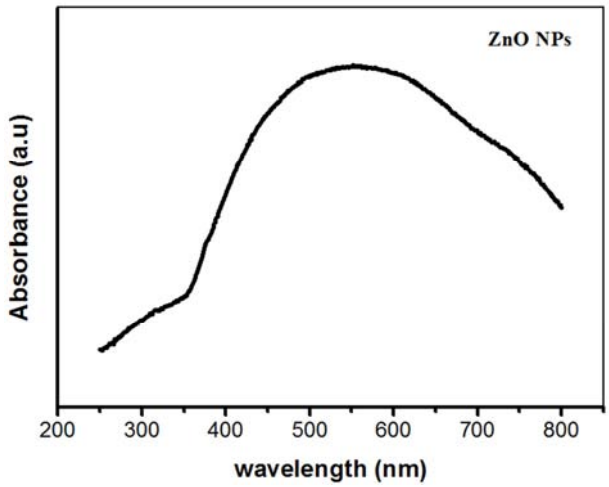

Figure 14. UV-vis absorbance spectrum of ZnO NPs.

The energy band gap (Eg) is calculated using the total active reflection coefficient (Tauc's) formula:

$$\text{Eg} = \frac{hc}{\lambda} \tag{3}$$

Where, Eg: Band gap energy (eV), Planks constant (h)=6.626×10^{-34}Joules sec, Velocity of Light (C)=2.99×10^{8} meter/sec and λ=Cut off wavelength=410.57×10^{-9} m or wavelength (λ)=Absorption peak value. Also 1 eV=1.6×10^{-19} Joules (Conversion factor), and if wavelength is given as 1 Angstrom=10^{-10} m [15], so energy band gap is given by:

$$\text{Eg} = \frac{1240.8}{\lambda(nm)} \tag{4}$$

λ: wavelength value (in nm), when λ starting point=250 nm, λ_{max}=550 nm, and last point=800 nm, the band gap energy values are (4.96, 2.26, 1.55) ev, which calculated according to ZnO NPs wavelength value respectively:

$$\text{Eg} = \frac{1240}{550} = 2.25\ ev \tag{5}$$

To correct determination of the band gap energy, the spectral dependence of the absorption coefficient for transitions between the allowed bands is described by relations:

$$\alpha = A\frac{(h\nu - Eg)^{½}}{h\nu} \tag{6}$$

$$\alpha = B\frac{(h\nu - Eg)^{2}}{h\nu} \tag{7}$$

The spectral dependences of absorption coefficient must linearize in so-called Tauc coordinates $(\alpha\cdot h\nu)^2$ – hν or $(\alpha\cdot h\nu)^{0.5}$ – hν for direct and indirect transitions, respectively. Where A and B are constants independent of wavelength. [16]

The optical band gap values of the ZnO, TiO_2 and composite ZnO/TiO_2 were obtain from the transmission measurements by plotting $(\alpha h\nu)^2$ versus photon energy graphs, where α is the absorption coefficient and hν is the photonic energy. When Origin program used to calculate the data, the energy band gap of ZnO NPs, which calculated from the carve value is 1.8 ev.

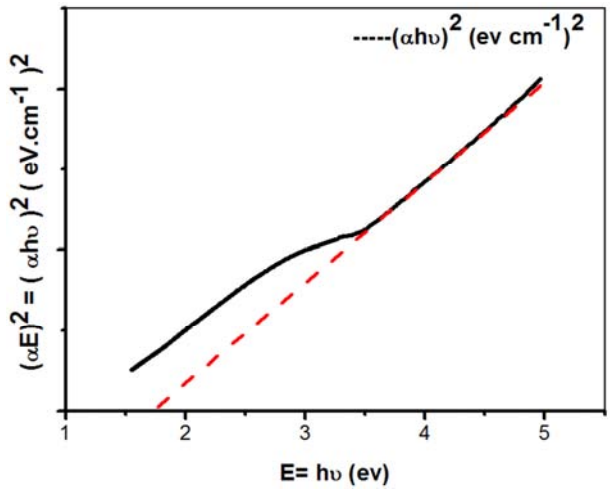

Figure 15. Tauc plot of synthesized ZnO NPs; it shows the variation of $((\alpha h\nu)^2$ vs. hν), having energy band gap (Eg)=1.8 eV.

The absorption of TiO_2 NPs starting in the wavelength 250 nm, calculation show the λ_{max} of TiO_2 NPs absorbance peak at 370 nm, the last point of absorption at 800 nm.

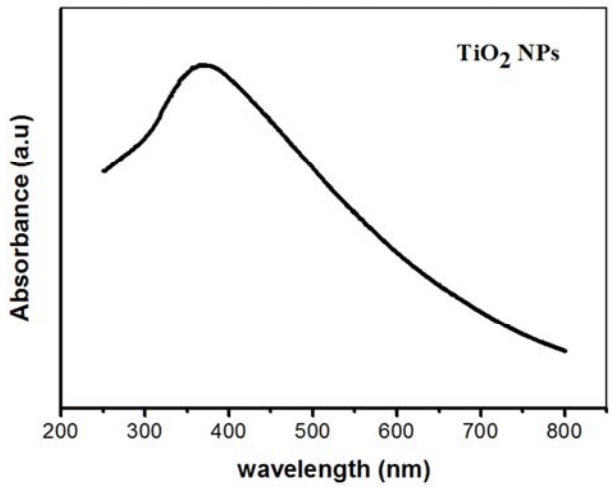

Figure 16. UV-vis absorbance spectrum of TiO_2 NPs, rutile.

Energy band gap are given by Tauc's formula (4), range are (4.96, 3.35, 1.55) ev, which calculated according to TiO_2 NPs wavelength value:

$$Eg = \frac{1240}{370} = 3.35\ ev \quad (8)$$

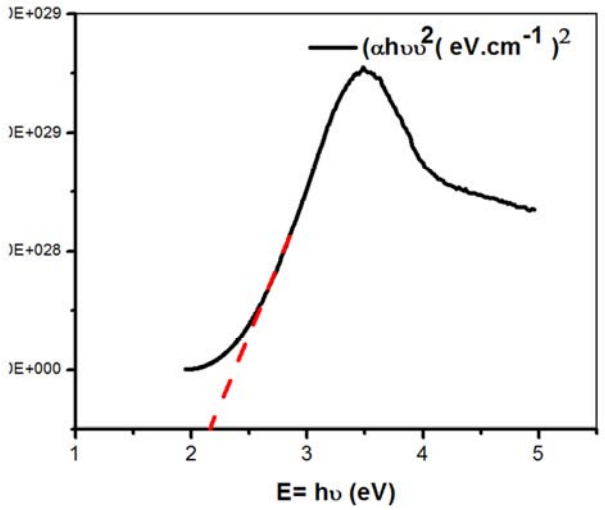

Figure 17. Tauc plot of synthesized TiO_2 NPs; having energy band gap (Eg)=2.2 eV.

Energy band gap of TiO_2 NPs calculated from the carve value is 2.2 ev, that means nanoparticle can be able to absorb visible wave length.

The absorption of composite ZnO/TiO_2 NPs starting in the wavelength at 250 nm, calculation show the λ_{max} of composite ZnO/TiO_2 NPs absorbance peak at 356 nm, the last point of absorbance at 800 nm.

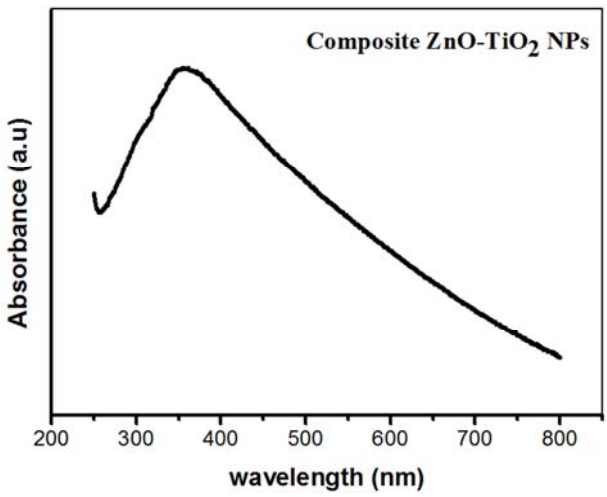

Figure 18. UV-vis absorbance spectrum of composite ZnO/TiO_2 NPs.

Energy band gap are given by Tauc's formula (4), range are (4.96, 3.48, 1.55) ev, which calculated according to composite ZnO/TiO_2 NPs wavelength value:

$$Eg = \frac{1240}{356} = 3.48\ ev \quad (9)$$

The energy band gap of composite ZnO/TiO_2 NPs calculated from the carve value is 2.25 ev.

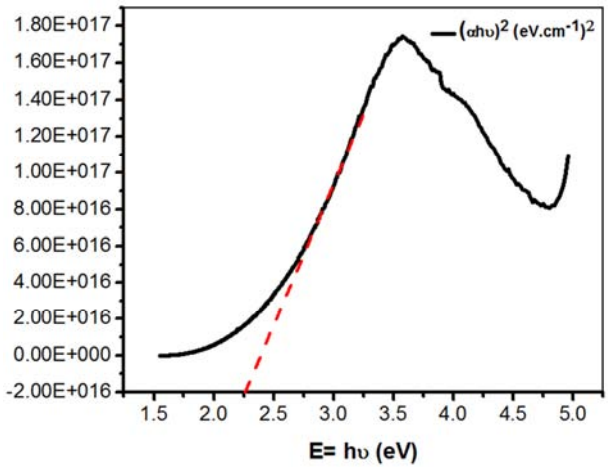

Figure 19. Tauc plot of synthesized composite ZnO/TiO_2 NPs; having energy band gap (Eg)=2.25 eV.

4. Conclusion

Bottom up approach was fundamental technique used to prepare nanomaterials, with low temperature chemical growth synthesized method. ZnO NPs, and composite ZnO/TiO_2 NPs has been successfully prepared by hydrothermal method, and they are attributed to their low production cost. The morphology and particle size are affected by its fabrication methods, it was experimentally proved that ZnO NPs have hexagonal shapes and the particles size are range between (111- 500) nm; TiO_2 NPs have a tetragonal shape and the particles size are range between (35- 50) nm, and composite ZnO/TiO_2 present as cubic NPs shape and the particles size are range between (36-53) nm. Lastly, UV-visible presented the wavelength absorbance peaks at (550, 370, 356) nm, and band gap range is reported to play important factor in determining the quality of NPs (1.8, 2.2, 2.25) eV of ZnO, TiO_2 and composite ZnO/TiO_2 NPs respectively in the samples. Advantages through understanding the preparation and characteristics of the composite ZnO/TiO_2, and ZnO photocatalyst in this study, produced under modification methods, can provide researchers with different perceptions towards photocatalysis results that can possibly be obtained, when their photocatalysts are integrated into different applications.

Acknowledgements

The authors would like to acknowledge colleagues from the National Centre for Research for excellence comments and suggestions in chemistry field, and Sudan University for Science and Technology- Materials Research Centre-Department of Micrographia laboratory, Also the Criminal Evidence especially the Department of physics for facility analysis of nanomaterials in their laboratory.

References

[1] I. J. ElSaliby, H. K. Shon, J. Kandasamy and S. Viganeswaran, Nanotechnology for Wastewater Treatment: in brief, water and wastewater treatment technologies, 2009, pp. 1, <http://www.eolss.net/EolsssampleAllChapter.aspx>.

[2] P. Pookmanee, I. Phiwchal, S. Yorlya, R. Puntharod, S. Sangsrichan, and S. Phanichphant, Titanium Dioxide (TiO_2) Nanopowder Prepared by the Low Temperature Solvothermal Method, *Ferroelectrics*, 2013, pp. 457: 30–38.

[3] Thomas Berger, Damin Monllor-Satoca, Milena Jankulovska, The Electrochemistry of Nanostructured Titanium Dioxide Electrodes, *Chem Phys Chem*, 2012, Vol. 13, no. 20, pp. 2824-2875.

[4] Min-HisnYeh, Lu-Yin Lin, Chen-Yu Chou, Chuan-Pei Lee, Hui-Min Chaung, R. Vittal, Kuo-ChaunHo, Preparing Core–Shell Structure of ZnO@TiO_2 Nanowires through a Simple Dipping–rinse–hydrolyzation Process as the Photoanode for Dye–Sensitized Solar Cells, *Nano Energy*, 2013, pp. 609- 620.

[5] Chin Boon Onga, Law Yong Ngb, Abdul Wahab Mohammad, A review of ZnO nanoparticles as solar photocatalysts: Synthesis, mechanisms and applications, *Renewable and Sustainable Energy Reviews*, 2018, pp. (536–551).

[6] Rupesh S. Devan, Ranjit A. Patil, Jin-Han Lin, and Yuan-Ron Ma, One-Dimensional Metal-Oxide Nanostructures: Recent Developments in Synthesis (Characterization and Applications), *Advanced Functional Materials*, 2012, Vol. 22, no. 22, pp. 3326–3370.

[7] Bing Wang, Shaohua Shen, Samuel S. Mao, Black TiO_2 for solar hydrogen conversion, *J Materiomics 3*, 2017, pp. 96-111.

[8] Shahram Moradi, Parviz Aberoomand-Azar, Sanaz Raeis-Farshid, Saeed Abedini-Khorrami, Mohammad Hadi Givianrad, activity of TiO_2/ZnO nano-composite, *Journal of Saudi Chemical Society*, 2016, issue 20, pp. 373–378.

[9] Qilin Li, Shaily Mahendra, Delina Y. Lyon, et al., Antimicrobial nanomaterials for water disinfection and microbial control: potential applications and complications, *water research*, 2008, pp. 4591-4602.

[10] P. Vlazan, D. H. Ursu, C. Irina-Mosiescu, I. Miron, P. SFirloaga, E. Rusu, structural and electrical properties of TiO_2/ZnO, Core shell nanoparticles synthesis by hydrothermal method, *Materials Characterization*, 2015, pp. 153-158.

[11] V. P. Dinesha, P. Bijia, Anuradha Ashoka, S. K. Dharab, M. Kamaruddinb, A. K. Tyagib and Baldev Raja, Plasmon-Mediated Highly Enhanced Photocatalytic Degradation of Industrial Textile Effluent Dyes using Hybrid ZnO@Ag Core-shell Nanorods, *The Royal Society of Chemistry*, 2014, pp. 1-16.

[12] Xu Y. N., Ching W. Y., Electronic, optical, and structural properties of some wurtzite crystals, Physical Review B 48, 1993, pp. 4335-4351.

[13] Meagher E. P., Lager G. A., Polyhedral thermal expansion in the TiO_2 polymorphs: Refinement of the crystal structure of rutile and brookite at high temperature sample at 25 degrees C, *The Canadian Mineralogist 17*, 1979, pp. 77-85.

[14] Verwey E. J. W., Heilmann E. L., Physical properties and cation arrangement of oxides with spinal structures, *Journal of Chemical Physics* 15, 1947, pp. 174-180.

[15] A. S. Bhadwal, R. M. Tripathi, R. K. Gupta, N. Kumar, R. P. Singh and A. Shrivastav, How to calculate optical band gap from UV spectra, *RSC Advances*, 2014, 4, pp. 9484-9490.

[16] Study of semiconductors by UV-Vis spectroscopy, Guidelines for laboratory work, Belarusian State University, TEMPUS program of the European Union, Project 530379-TEMPUS-1-2012-1-LVTEMPUS-JPCR, 2012.